



## **ANALYSIS OF TRACER TESTS WITH MULTIRATE DIFFUSION MODELS: RECENT RESULTS AND FUTURE DIRECTIONS WITHIN THE WIPP PROJECT**

Sean A. McKenna, Lucy C. Meigs, Susan J. Altman,  
Sandia National Laboratories, Albuquerque, New Mexico, U.S.A.

Roy Haggerty  
Oregon State University, Corvallis, Oregon, U.S.A

### **Abstract**

A series of single-well injection-withdrawal (SWIW) and two-well convergent-flow (TWCF) tracer tests were conducted in the Culebra dolomite at the WIPP site in late 1995 and early 1996. Modeling analyses over the past year have focused on reproducing the observed mass-recovery curves and understanding the basic physical processes controlling tracer transport in SWIW and TWCF tests. To date, specific modeling efforts have focused on five SWIW tests and one TWCF pathway at each of two different locations (H-11 and H-19 hydropads).

An inverse parameter-estimation procedure was implemented to model the SWIW and TWCF tests with both traditional and multirate double-porosity formulations. The traditional model assumes a single diffusion rate while the multirate model uses a first-order approximation to model a continuous distribution of diffusion coefficients. Conceptually, the multirate model represents variable matrix block sizes within the Culebra as observed in geologic investigations and also variability in diffusion rates within the matrix blocks as observed with X-ray imaging in the laboratory. Single-rate double-porosity models cannot provide an adequate match to the SWIW data. Multirate double-porosity models provide excellent fits to all five SWIW mass-recovery curves. Models of the TWCF tests show that, at one location, the tracer test can be modeled with both single-rate and multirate double-porosity models. At the other location, only the multirate double-porosity model is capable of explaining the test results.

## Introduction

A number of single-well injection-withdrawal (SWIW) and two-well convergent flow (TWCF) tracer tests have been conducted in the Culebra Dolomite member of the Rustler Formation in the vicinity of the Waste Isolation Pilot Plant (WIPP) in southeastern New Mexico. These tracer tests were conducted with the goal of better characterizing the physical transport parameters of the Culebra dolomite and the test results are summarized in Meigs and Beauheim [in prep].

The Culebra Dolomite is roughly 7 meters thick in the area of the WIPP site. The Culebra represents a potential pathway for off-site migration of radionuclides under the scenario of human intrusion into the repository. The Culebra is well fractured and, for the modeling results presented herein, the hydraulic conductivity can be considered as an effective continuum. The transport properties of the Culebra are conceptualized as a double-porosity system with advection through the connected fractures and solute storage occurring in the matrix blocks and in dead-end fractures.

The goal of this paper is to elucidate the processes responsible for mass transfer in the Culebra Dolomite. Toward this goal, we are interested in developing a model of mass transfer between fracture and matrix porosity, or more generally between advective porosity and diffusive porosity, and testing that model on data acquired in a number of SWIW and TWCF tracer tests.

### 1.1 Mathematical Model

The multirate model [Haggerty and Gorelick, 1998] enables mass transfer to be modeled with a continuous distribution of diffusion rate coefficients. Variability in matrix block sizes and tortuosity can cause a distribution of diffusion rate coefficients. For sorption processes, mass transfer is viewed as a first-order surface reaction. The surfaces involved may be those accessed by advection, diffusion or some combination of these transport processes. Total mass transfer within an aquifer can be any combination or probability density function of diffusion or surface reaction processes [Haggerty and Gorelick, 1995].

In this paper, we are concerned solely with diffusion processes and interpretation of tracer tests done with non-sorbing tracers (benzoic acids). The multirate mass transfer model presented here is similar to that described by Cunningham *et al.* [1997] and Haggerty and Gorelick [1998]. Diffusion is assumed to occur along one-dimensional pathways within the matrix blocks, and it is assumed that mass-transfer properties are homogeneous along each pathway and that the pathways are independent of one another. The pathways and matrix blocks can be any shape as long as the diffusion rate coefficients form a continuous distribution. In this work, we employ a log-normal distribution of diffusion rate coefficients for reasons discussed in Haggerty and Gorelick [1998].

The equations for solute transport into or out of a well, in the presence of a lognormal distribution of matrix diffusion processes, is given by (after Haggerty *et al.* [in press]):

$$\frac{\partial c_a}{\partial t} + \int_0^{\infty} \beta(\alpha_d) \frac{\partial \hat{c}_d(\alpha_d)}{\partial t} d\alpha_d = \frac{1}{r} \frac{\partial}{\partial r} \left( \frac{r\alpha_L |v|}{R_a} \frac{\partial c_a}{\partial r} \right) - \frac{v}{R_a} \frac{\partial c_a}{\partial r} \quad (1)$$

$$\beta(\alpha_d) = \frac{\beta_{tot}}{\sqrt{2\pi}\sigma_d\alpha_d} \exp\left\{-\frac{[\ln((\alpha_d) - \mu_d)]^2}{2\sigma_d^2}\right\} \quad (2)$$

where:

$$\alpha_d = \frac{D_a}{l^2} \quad (2b)$$

and

$$\beta_{tot} = \frac{\phi_d R_d}{\phi_a R_a} \quad (2c)$$

and where  $c_a$  [M/L<sup>3</sup>] is the solute concentration in the advective porosity (e.g. fractures);  $\bar{c}_d$  [M/L<sup>3</sup>] is the average solute concentration in the portion of the matrix associated with a particular diffusion rate coefficient;  $\alpha_d$  [1/T] is the diffusion rate coefficient described in (2b), which is continuously distributed;  $\beta(\alpha_d)$  [-] is the capacity coefficient as a function of the diffusion rate coefficient probability density function (PDF). We assume the diffusion rate coefficient PDF to be lognormal in (2a);  $\beta_{tot}$  [-] is the total capacity coefficient of the formation, which is the ratio of mass in the matrix to mass in the fractures at equilibrium;  $v$  [L/T] is the pore-water velocity;  $R_a$  [-] is the retardation factor in the advective porosity;  $r$  [L] is the radial coordinate (positive away from well);  $t$  [T] is time elapsed since the beginning of injection of the first tracer;  $\sigma_d$  is the standard deviation of the log-transformed diffusion rate coefficients;  $\mu_d$  is the natural log of the geometric mean of the diffusion rate coefficients;  $D_a$  [L<sup>2</sup>/T] is the apparent diffusion coefficient in the matrix, which may be defined most simply as the product of the aqueous diffusion coefficient of the tracer and diffusive tortuosity, although this expression may be modified to incorporate processes such as immobile zone sorption;  $l$  [L] is the length of the diffusion pathway within the matrix;  $\phi_d$  [-] is the diffusive porosity of the formation; and  $R_d$  is the retardation factor due to sorption within the diffusive porosity;  $\phi_a$  [-] is the advective porosity. Equations describing the concentration distribution within the diffusive porosity along with boundary conditions for the solution of these equations in SWIW and TWCF systems are discussed in *Haggerty et al.* [in prep] and *McKenna et al.*, [in prep].

Detailed examination of geology in many subsurface environments suggests that a distribution of mass-transfer rates arising from variation in block sizes is geologically more plausible than the single matrix block size ("sugar cube") conceptualization employed in standard double porosity models (Figure 1). Equation 2 not only defines this distribution of diffusion rate coefficients, assumed to be lognormal in this work, but provides a critical link between the diffusion rate coefficients and the solute storage capacity of the diffusive porosity associated with each rate coefficient. Equation 2 ties each diffusion rate coefficient,  $\alpha_d$ , to a specific volume of storage. This volume is specified as a fraction of the total storage capacity of the medium,  $\beta_{tot}$ , and is expressed as a function of the diffusion rate coefficient  $\beta(\alpha_d)$ . At equilibrium conditions,  $\beta_{tot} = \phi_d / \phi_a$ . Also, it is noted that in (2b) variability in  $\alpha_d$  is due to variability in both  $l$  and  $\tau$  and that the joint variability cannot be further refined.

## 1.2 Damkohler Number

For a given experimental setup and duration, the diffusive impacts of only a limited range of block sizes can be investigated directly. The ability of the multirate model to estimate the diffusion rate coefficient distribution is limited by the ratio of diffusive to advective mass-transfer rates within the tracer test system. The ratio of diffusive to advective mass transfer can be parameterized with the (dimensionless) type I Damkohler number,  $DaI$ . For a one-dimensional flow system with first-order diffusive mass transfer into layers, the type I Damkohler number is [after, *Haggerty and Gorelick, 1995*]:

$$DaI = 3\alpha_d(\beta(\alpha_d) + 1) \frac{RL}{\bar{v}} \quad (3)$$

where  $L$  [L] is the transport length and  $\bar{v}$  [L/T] is the average velocity along the transport path. Damkohler numbers near 1 indicate that the rate of diffusion is similar to the rate of advection. At a Damkohler number of 100 or larger, diffusion can be considered instantaneous relative to advection and the local equilibrium assumption (LEA) applies [*Bahr and Rubin, 1987*]. In this situation, the porosity available for solute transport is equal to  $(\phi_a + \phi_d)$ . Conversely, at a Damkohler number of 0.01 or smaller, diffusion is negligible relative to advection at the time and geometric scales of interest, and a single porosity ( $\phi_a$ ) numerical implementation of the overall conceptual model for transport will be adequate.

The Damkohler number can be examined across the distribution of mass-transfer rates in a radial flow system by considering the average velocity along a flowpath from an arbitrary starting radius,  $R_o$ , to the extraction well radius,  $r_w$  ( $L = R_o - r_w$ ). We apply the Damkohler number limits to the TWCF test data to determine the resolution of the tests in terms of defining diffusion rate coefficients.

## Simulation of Tracer Test Data

Five SWIW and two pumping-injection well pairs are analyzed. Both types of tests were conducted at the H-11 and H-19 hydropads near the WIPP site. The different benzoic acid tracer tests will be referred to by the hydropad. All fluid and tracer injection and withdrawals were done across the full aquifer thickness. Further details regarding the physical setup and data collection of the tracer tests can be found in *Meigs and Beuheim* [in prep].

The SWIW tests were accomplished by injecting a tracer and a Culebra-brine chaser into the Culebra. After a rest period of approximately 17 hours, the well was pumped and the discharge was sampled for up to 1000 hours to determine the mass recovery curve. Two TWCF tests are considered here. The H-11 test was run at a constant pumping rate for approximately 25 days after injection of the tracer. During this time period, 107 samples were collected and analyzed for concentration. For the H-19 tracer test, 67 samples were collected during a pumping period of 29 days.

## 2.1 Parameter Estimation

Parameter estimation applied to the multirate diffusion model discussed above is used to provide an optimal fit of the model to the observed data. The parameter estimation minimizes the root mean square error (RMSE) between the log of the observed data and the log of the predicted concentration. Four parameters are estimated: the mean ln diffusion rate coefficient,  $\mu_d$ , the standard deviation of the ln diffusion rate coefficient distribution,  $\sigma_d$ , the advective porosity,  $\phi_a$ , and the longitudinal dispersivity,  $\alpha_l$ . The parametric expression of diffusion rate coefficients used here is a log-normal distribution which is fully characterized by its mean and standard deviation. The estimated parameter values and the RMSE statistic obtained with the multirate model are given for the H-11 and H-19 tests in Table 1. Modeled results are shown with the observed data in Figures 2A and 2B for the H-11 and H-19 SWIW tests and in Figure 3 for the H-11 and H-19 TWCF tests.

Results shown in Figures 2 and 3 are based on estimated log-normal distributions of diffusion coefficients. The cumulative matrix volumes as a function of diffusion rate coefficient as determined from the inverse parameter estimation using the multirate model are shown in Figures 4A and 4B for both the SWIW and TWCF tests. Examination of Figure 4 shows that there is a large difference in the distributions between the H-11 and H-19 hydropads. For both types of tests, the standard deviation of the diffusion coefficient distribution is much larger at H-19 than at H-11.

## 2.2 Resolution of Tracer Tests

The portion of the log-normal distributions that can actually be resolved during the tests is determined by applying the Damkohler number limits of 0.01 and 100. The changing flow velocities and rest period of the SWIW test make calculation of the Damkohler limits quite complex. Here we use a conservative approximation of those limits as described in Haggerty et al [in prep.]. As shown in Figure 4A, the SWIW tests show that roughly 80 percent of the diffusion rate coefficient distribution lies within the Damkohler limits at the H-11 hydropad. For the H-19 SWIW tests, approximately 70-80 percent of the distribution lies within the limits.

For the TWCF tests, the H-11 hydropad has roughly 85 percent of the diffusion rate distribution within the 0.01 and 100 Damkohler number limits, while at the H-19 hydropad approximately 55 percent of the distribution lies within the limits (Figure 4B). Consequently, at the H-19 hydropad approximately 30 percent of the estimated diffusion rates are so small as to be negligible and approximately 15 percent of the rates are fast enough to appear instantaneous. The distribution of diffusion coefficients is effectively inestimable outside these Damkohler limits and only has shape in those regions because of the *a priori* assumption of a log-normal distribution.

The consistency of the estimated, log-normal distributions of mass-transfer rates can be checked by determining the estimated matrix block size distribution. All variability in the mass transfer rates can be assigned to variations in matrix block size by assuming a constant tortuosity and then comparing estimated matrix block lengths to field observations. For one-dimensional diffusion paths into the matrix, it is possible to calculate the distance from the fracture/matrix interface to the center of the matrix block,  $l$ , (matrix block 1/2 length) by rearranging equation (2b). Using measured values of aqueous diffusion coefficient,  $D_o$ , and average values of  $\tau$  as measured in core samples (0.09 at H-11

and 0.11 at H-19), solution of equation (2b) shows that the SWIW are capable of resolving block sizes from  $< 2 \times 10^{-04}$  meters to 0.20 meters. The TWCF tests were able to resolve, within the Damkohler limits, a range of half-block sizes from  $< 0.001$  to 0.13 meters at the H-11 hydropad and from 0.002 to 0.13 meters at the H-19 hydropad. These estimates of block size are consistent with the lower end of the range of block sizes observed in core and outcrop samples [Holt, 1997].

Previous to this work, only single-valued diffusion rates have been applied to the analysis of two-well, double porosity tracer tests. To compare the results of the multirate model to the traditional, single-rate (double porosity) approach, single-rate model runs were completed using parameter estimation for the tracer tests at each hydropad. This estimation procedure is the same as that used for the multirate model; however,  $\sigma_d$  is set to 0.0. In order to maintain consistency, these single-rate runs were constrained to have the same total porosity ( $\phi_a + \phi_d$ ) as derived from the multirate modeling. Results of the single-rate matches to the observed data are given in Table 2 and Figures 5A and 5B. Note that single-rate solutions could only be obtained for two of the five SWIW tests.

In general, the single-rate of mass transfer is smaller (larger negative number) than the mean of the multirate distribution for both of the TWCF tests modeled. The estimated mass-transfer rate using the traditional double-porosity model results in matrix half-block sizes of 0.11 and 0.03 meters in the SWIW tests and 0.18 and 0.33 meters at the H-11 and H-19 hydropads respectively. Additionally, the advective porosity estimated with a single-rate model is higher than that estimated with the multirate model. For the H-19 TWCF test, this increase in  $\phi_a$  is over an order of magnitude (Table 2). As measured by the RMSE, the multirate model provides a significantly better fit to the data than does the single-rate model for all tests with the exception of the H-19 TWCF test. The RMSE of the single-rate model fit for the H-19 TWCF test is only slightly higher than that obtained with the multirate model.

## Conclusions

The multirate diffusion model developed previously for one-dimensional flow [Haggerty and Gorelick, 1995] is extended to the case of a convergent flow system with a injection at radial distance from the pumping well. This model has been applied to the results of the H-11 and H-19 tracer tests conducted in the Culebra dolomite at the WIPP site. Model results show significant differences in the diffusion process at the two hydropads. At the H-11 hydropad, the multirate diffusion model is necessary to describe the breakthrough curve.

Models developed with data from a SWIW test are not necessarily transferable to a TWCF test. The fast end of the diffusion rate distribution is better estimated with a SWIW test because of the insensitivity of that test to advective porosity. The portion of advective porosity that is due to instantaneous diffusion rates or in fact is actually fracture porosity, may be indeterminate in a TWCF test. At H-19, the insensitivity of the SWIW test to advective porosity made it impossible to model that test with a single-rate model. However, it is possible to model the H-19 TWCF with an increased advective porosity to account for the instantaneous diffusion and fit the data with a single-rate model.

In the TWCF tests at the H-19 hydropad, the choice of a conceptual model (multirate over single-rate) is non-unique. Both models did an adequate job of fitting the TWCF test. Calculation of Damkohler numbers across the distribution of diffusion coefficients shows that roughly 50 percent of the estimated distribution is beyond the resolution of the tracer test and thus cannot be estimated with any confidence. The single-rate model can be viewed as a multirate model with two discrete mass-transfer rates: instantaneous and extremely slow. The instantaneous rates are modeled in a single-rate model as advective porosity and the single-rate is estimated to be very slow (infinite block size). More work is necessary to determine if multi-modal or other non-parametric distributions can be used to model the tracer breakthrough curves at H-19.

## Acknowledgements

Sandia is a multiprogram laboratory operated by Sandia Corporation, a Lockheed Martin Company, for the United States Department of Energy under Contract DE-AC04-94AL85000. Some calculations herein were done by M. Kelley, T. Jones and J. Ogintz.

## References

- Bahr, J.M., and J. Rubin, 1987, Direct comparison of kinetic and local equilibrium formulations for solute transport affected by surface reactions, *Water Resour. Res.*, 23(3), pp. 438-452.
- Cunningham, J.A., C.J. Werth, M. Reinhard and P.V. Roberts, 1997, Effects of grain-scale mass transfer on the transport of volatile organics through sediments, *Water Resour. Res.*, 33(12), 2713-2726.
- Haggerty, R., S.W. Fleming, L.C. Meigs, S.A. McKenna, (in prep.), Convergent-flow tracer tests in a fractured dolomite, 3, Analysis of mass transfer in single-well injection-withdrawal tests, for submission to *Water Resour. Res.*
- Haggerty, R., and S. M. Gorelick, 1998, Modeling mass transfer processes in soil columns with pore-scale heterogeneity, *Soil Sci. Soc. Am. J.*, 62(1), 62-74.
- Haggerty, R. and S.M. Gorelick, 1995, Multiple rate mass-transfer for modeling diffusion and surface reactions in media with pore-scale heterogeneity, *Water Resour. Res.*, 31 (10), 2383-2400.
- Holt, R.M., 1997, Conceptual model for transport processes in the Culebra Dolomite Member, Rustler Formation, SAND97-0194, Sandia National Laboratories, Albuquerque, NM.
- McKenna, S.A., L.C. Meigs and R. Haggerty, (in prep.), Tracer tests in a fractured dolomite 4. Double porosity, multiple-rate mass transfer processes in two-well convergent flow tests, for submission to *Water Resour. Res.*
- Meigs, L.C. and R.L. Beauheim, (in prep.), Tracer tests in a fractured dolomite, 1, Experimental design and observed tracer recoveries, for submission to *Water Resour. Res.*

**Table1:** Parameters estimated with the multirate model on SWIW and TWCF tests.

Test	Estimated Parameters				
SWIW	$\phi_{adv}$	$\alpha_l$	$\mu_d$	$\sigma_d$	RMSE
H11-1	1.6x10-03	0.06	-16.5	3.6	0.18
H11-2	4.7x10-03	0.07	-16.0	3.8	0.26
H19S2	1.1x10-02	0.18	-10.6	5.7	0.15
H19S1-1	4.9x10-03	0.21	-11.9	6.9	0.08
H19S1-2	2.1x01-02	0.12	-10.1	2.64	0.17
TWCF					
H-11(L)	8.1x10-04	3.4	-17.6	1.3	0.10
H-19(L)	3.8x01-03	1.0	-16.2	5.5	0.11

**Table 2:** Parameters estimated with the single-rate model on SWIW and TWCF tests. It was not possible to fit three of the SWIW tests with a single-rate model.

Test	Estimated Parameters				
SWIW	$\phi_{adv}$	$\alpha_l$	$\mu_d$	$\sigma_d$	RMSE
H11-1	7.1x10-03	0.46	-18.8	0.0	0.51
H19S1-1	5.4x10-02	0.16	-16.2	0.0	1.21
TWCF					
H-11(L)	1.5x10-03	0.9	-19.8	0.0	1.83
H-19(L)	5.7x10-02	2.4	-21.1	0.0	0.16

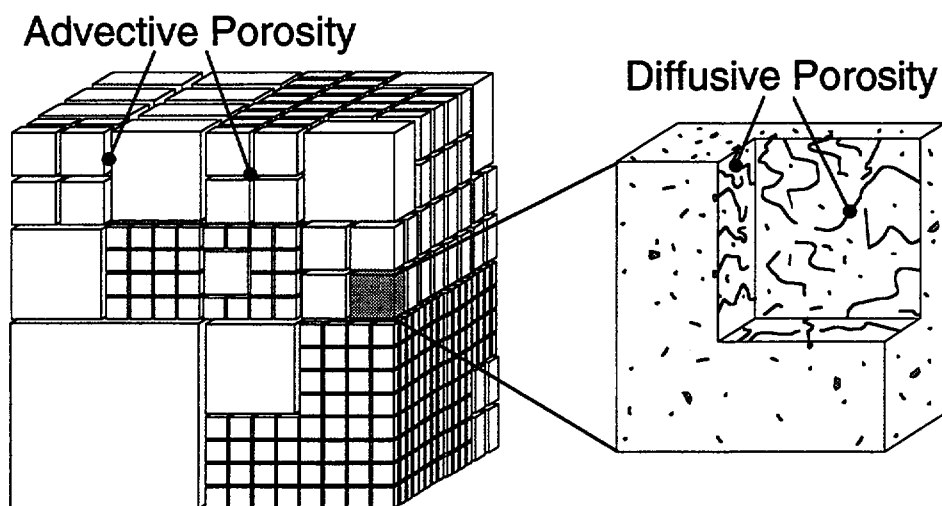


Figure 1. Conceptual model for multirate diffusion.

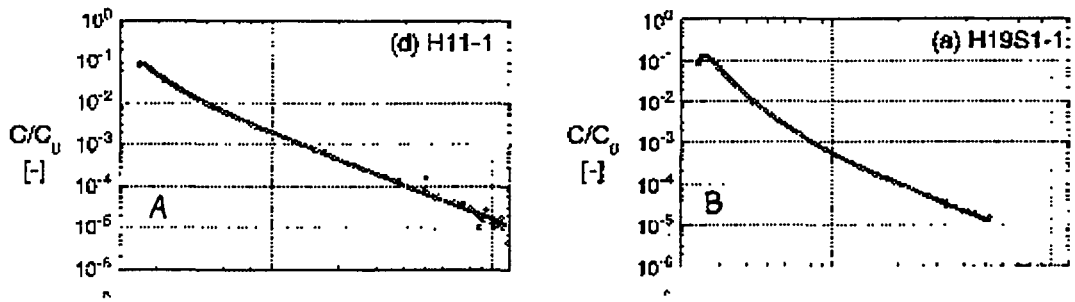


Figure 2. SWIW data and multirate model fits to the data for A) H-11 and B) H-19.

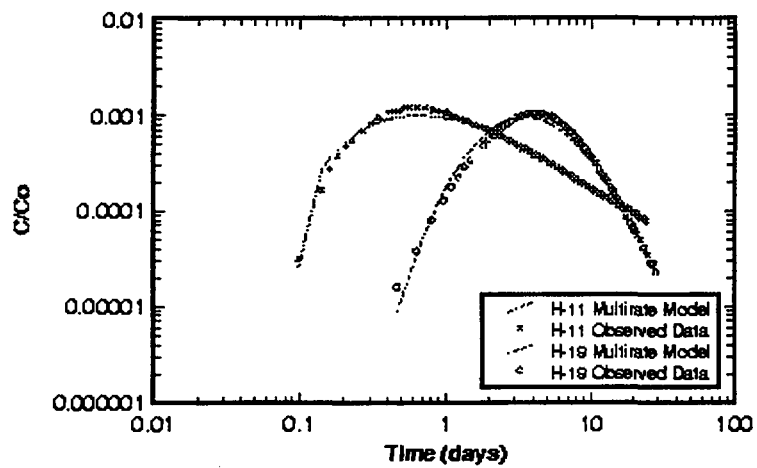


Figure 3. TWCF data and multirate model fits to the data for H-11 and H-19.

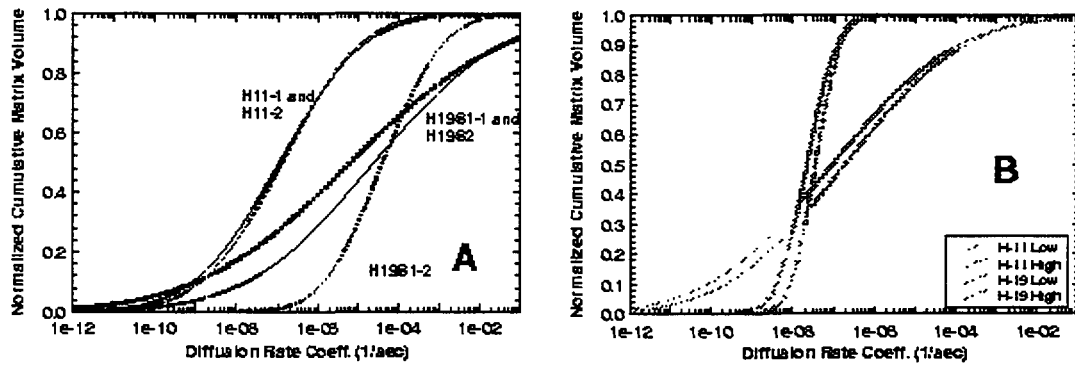


Figure 4. Cumulative distributions of diffusion rate coefficients as determined with the multirate model for the (A) SWIW tests and (B) TWCF tests. The Damkohler limits are defined by the vertical dotted lines in (A) and the bold portion of the lines in (B).

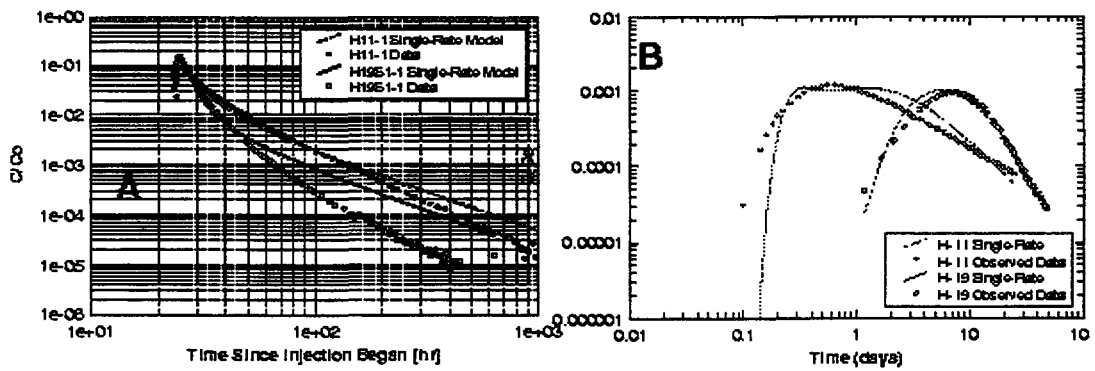


Figure 5. Single-rate model fits to the (A) SWIW tests and (B) the TWCF tests. Note that single-rate models could only be obtained for two of the SWIW tests.